MODIFIED AC MAGNETIC BRIDGE SCANNING PATTERNS OF SAMPLES SIMULATING FLAWS IN AIRCRAFT SEAMS

Otto H. Zinke[1] and William F. Schmidt[2]
[1]Physics Department
[2]Mechanical Engineering Department
University of Arkansas, Fayetteville
Fayetteville, Ar 72701

Hidden corrosion in the seams or below the skin of an aluminum aircraft results in the loss of material and therefore affects the net conductance as measured at the seam or skin surface. This loss of conductance has been detected through the use of electromagnetic techniques, for example, eddy-current techniques [1].

The results of preliminary tests of an electromagnetic technique involving a modified electromagnetic bridge on simulated corrosion losses are described here. The modified AC magnetic bridge has been used for a variety of nondestructive tests [2]. The tests results presented in this paper are preliminary for a number of reasons: 1. The corrosion loss was simulated by removing material with an end mill. 2. The plates simulating the seams were flat rather than gently rounded. 3. There was no variable lift-off problem such as would be seen on the roughened skin of aging aircraft. (However, the paint on such aircraft should have little effect on these measurements.) The bridge was operated at a lift off of 0.008 inches. 4. No tests were made of the limits of scanning speed. 5. No attempt was made to either optimize the design of the gaps in the bridge or to choose a more appropriate frequency. The bridge was operated at 1.92 Khz.

The rounded skin mentioned in Item 2. above can be accommodated by grinding the bridge head to fit. It appears that the variable lift off can be corrected both through data processing (as shown here) and possibly through phase/amplitude correlations. From other experiments the lower limit of scanning speeds has been estimated to be of the order of feet per second. Recently, a model of the electromagnetic field of the bridge gap has been developed [2] which may allow optimization of the gap design both with respect to sensitivity and to minimizing lift-off effects. With lower frequencies, the electromagnetic fields should penetrate more deeply into the samples.

Review of Progress in Quantitative Nondestructive Evaluation, Vol. 12
Edited by D.O. Thompson and D.E. Chimenti, Plenum Press, New York, 1993

The aircraft skin was simulated by an aluminum plate which was 7 by 10 inches by 0.047-inches thick; a drawing of which is shown in Fig. 1. Corrosion was simulated by using a 3/8 inch end mill to remove material. Three states were considered by milling 0.009, 0.006, and 0.003 inches deep accounting for material losses of 19, 13, and 7 percent at x=3, 5, and 7 inches respectively. Aircraft seams were simulated by combining this plate with another plate the same size but with no material removed. Two types of scans were taken, one over areas of the plates representing scans over unflawed areas shown as Scan A in Fig. 1 and scans over flawed areas shown as Scan B in Fig. 1. Scans were taken over the milled plate alone as shown in a. of Fig. 2 which represented hidden corrosion under the skin. Scans of the two plates arranged as shown in b.,c. and d. of Fig. 2 represent hidden corrosion between and under the seams. Measurements were made every 1/4 inch on each scan. The position of the bridge relative to the plates is represented by Z in Fig. 2.

AC magnetic bridges require the adjustment of two electrical parameters for nulling just as AC electrical bridges do. These parameters are generally resistance (R) and capacitance (C) just as with AC electrical bridges. However, with magnetic bridges, the resistances and capacitances are electrically connected in parallel to coils around the bridge arms, see e.g. Zinke and Schmidt [3] or Zinke and Derby [4]. From the resistances and capacitances required to renull the bridge, real (R_e) and imaginary (R_I) reluctances can be calculated as follows [5]:

$$R_e = N^2 \omega^2 C \quad \text{and} \tag{1}$$

$$R_I = - N^2 \omega / R \tag{2}$$

where ω is the angular frequency and N is the number of turns of the coil wound on the bridge arm. When the bridge is renulled by adjusting the resistances and capacitances at each measuring point, the bridge is said to be operated in the renull mode, and the

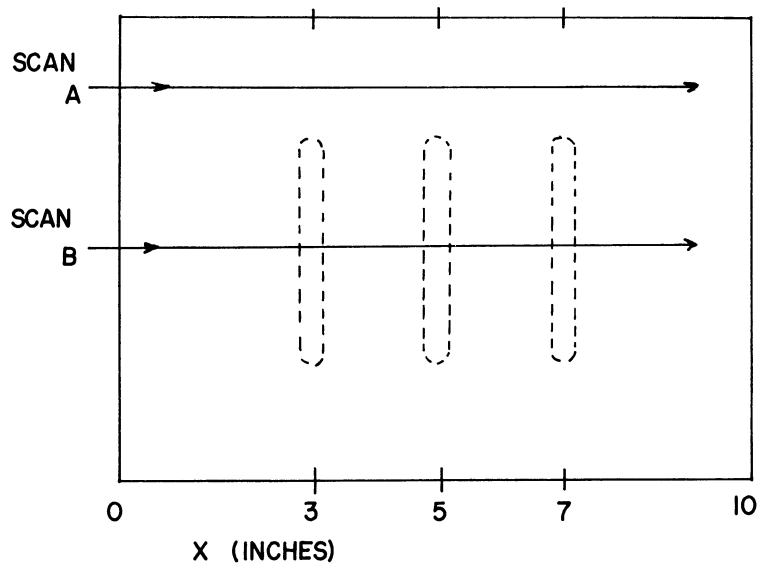

Fig. 1. Sample simulating corrosion loss on aircraft skin.

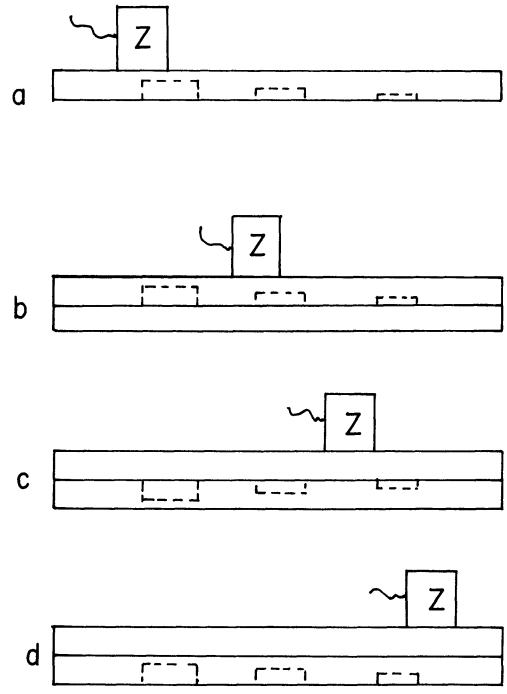

Fig. 2. Plates and bridge configurations.

above equations are used. The bridge can also be operated in the off-null mode. In the off-null mode, the bridge is nulled by adjusting the resistance and capacitance attached to the bridge at some place on the sample (x=2, Scan A in these experiments), and those values of resistance and capacitance remain fixed as the bridge is moved from point to point for measurements. The off-null values of voltage and phase can then be recorded for each measurement. Data from both off-null and renull modes are presented here. The off-null data are presented as measured.

In the off-null mode, the deviations from null of the voltage and the phase are produced by changes in the real and imaginary reluctance of the sample. To show how off-null voltages and phases might change, the imaginary reluctance changes of the sample were simulated by nulling the bridge at one point on the sample. The capacitance was then held constant, and the resistance was changed while the off-null voltage and phase were recorded. Typical variations of the output voltages and phases of the bridge versus changes in the imaginary reluctance, for example, are shown in Fig. 3. The off-null voltages varied between 0 and 1,000 millivolts, and the off-null phase varied between -125 and 50 degrees. Note the rapidity at which the off-null phase changes through null (approximately 180 degrees for very small changes in reluctance) as compared to the off-null voltage.

The detection of flaws with an electromagnetic device in the field usually depends on the comparison between flawed and unflawed regions of the specimen. Data processing is based on this fact. The data from unflawed scans are important because they are representative of lift-off problems and, in this case, potential problems with varying space between the two sheets of aluminum representing the seams. Scan A is the unflawed scan. The resistances and capacitances required to null the bridge were obtained every 1/4 inch along Scan A for the configurations a, b, c, and d of the

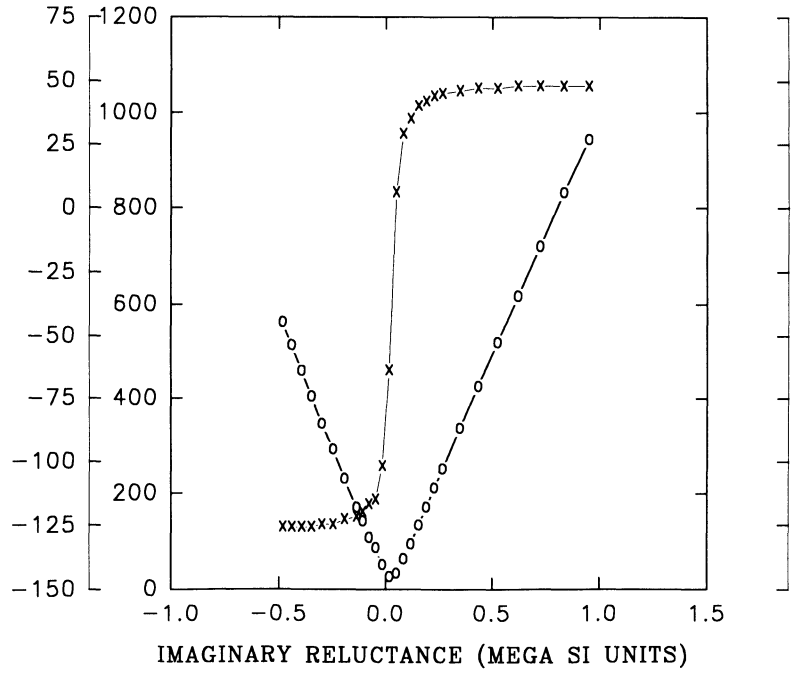

Fig. 3. Variation of off-null voltage (0-curve) and off-null phase (X-curve) with imaginary reluctance.

plates as seen in Fig. 2. The associated values of the real and imaginary reluctance were calculated for each measurement. These values were then averaged for each plate configuration producing averages of real and imaginary reluctance for each of the configurations a, b, c, and d. The units of these reluctances were in amperes/weber. Finally, the real and the imaginary reluctances were multiplied together to produce the curves marked by circles in Figs. 4 and 9. The values resulting from this are referred to as "processed data." No theoretical justification is offered for the multiplication procedure. The individual reluctance curves where the reluctances were not multiplied showed variations similar to those seen in off-null data associated with the scans of the same plate configurations. It is apparent from comparisons between the processed data and the off-null curves that the multiplication procedure minimized the effects of variations which were suspected to arise either from variable lift off or from variations in the distance between the plates representing the seam. Scan B is over the center of the flaws. The values of resistance and of capacitance required for null were taken in intervals of 1/4 inch for a B scan for each plate configuration. Real and imaginary reluctances were calculated for each of these measurements. Then the average Scan A real reluctance were subtracted from each real reluctance value obtained in Scan B. The same calculation was made for the imaginary reluctance. Both of these sets of calculations were repeated for plate configurations b, c, and d. Finally, the real reluctance and the imaginary reluctance for each B scan were multiplied together. The results appear as crosses in Figs. 4 through Fig. 9.

In Fig. 4A, the processed renull data for both Scan A and Scan B are displayed. The scans were for the configuration representing the skin with hidden corrosion (Fig. 2a). In Fig. 4B, the unprocessed, off-null voltages for both scans are displayed. The

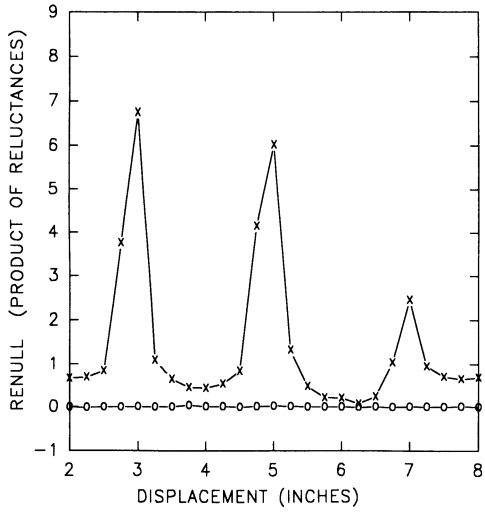

Fig. 4A. Scan of simulated hidden flaws under aircraft skin.

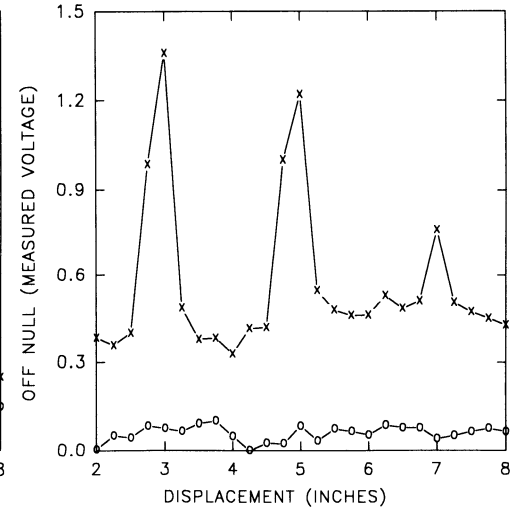

Fig. 4B. Scan of simulated hidden flaws under aircraft skin.

Scan A results are shown as O's, and the Scan B results are shown as X's. This same convention is used throughout the rest of the paper. The response to the 19, 13, 7 percent material losses appear at 3, 5, and 7 inches respectively. Note that the data processing greatly reduces the excursions in the unflawed renull scan of Fig. 4A as compared to the unprocessed, off-null, unflawed scan of Fig. 4B.

In Figs. 5A and 5B, results similar to those of Figs. 4A and 4B are presented for simulated corrosion which would occur at the interface of a seam with corrosion above the interface. The configuration is shown in Fig. 2b. The renull curves of Fig. 5A again indicate the presence of the 19, 13, and 7 percent losses at x=3, 5, and 7 inches, but in the off-null data, the failure of a response to the 7 percent loss represents a problem with off-null data of Fig. 5B. Previously it was pointed out that the resistances and capacitances for the off-null data were set at a particular point on Scan A. There is the possibility that this point will not be representative of the average conditions of one of the B scans, particularly where the spacing between the plates may differ somewhat between the null point and the average on the B scans. Thus, the curves of Fig. 3, may not be centered at the point of zero reluctance for the B scan, but may be set slightly to one side or the other. This offset will be referred to as a "bias" here. If the bridge is biased near the null in setting the standard null condition as it was here, small responses in the voltage data can be lost. That this was the case can be seen in Fig. 6 which presents the off-null phase for this scan. Note that all three losses are detected in this phase scan at much the same amplitude, indicating (from Fig. 3) that the bridge must have been nulled in the standard condition very near the null for Scan B. However, using the off-null phase does not necessarily guarantee more reliable detection as can be seen from Fig. 7 where the off-null phase of Scan B is shown for the skin alone (Fig. 2a). In the phase scan of Fig. 7, no indications are seen

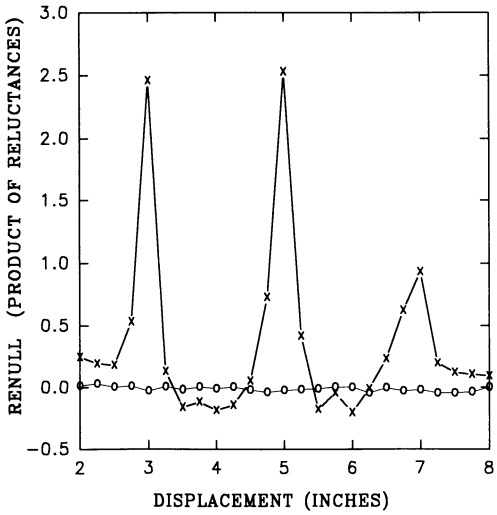

Fig. 5A. Scan of simulated hidden corrosion on the underside of outside plate of seam.

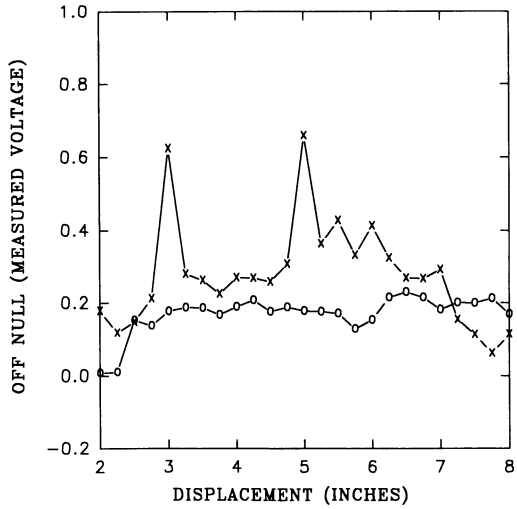

Fig. 5B. Scan of simulated hidden corrosion on the underside of outside plate of seam.

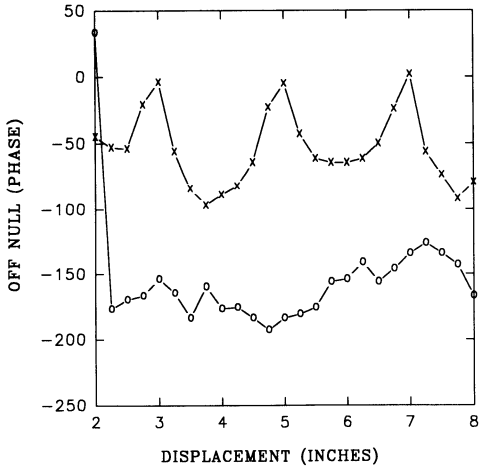

Fig. 6. Scan of simulated hidden corrosion on the underside of outside plate of seam.

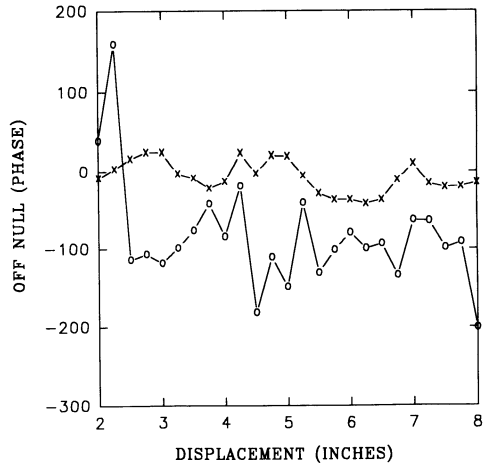

Fig. 7. Scan of simulated hidden flaws under aircraft skin.

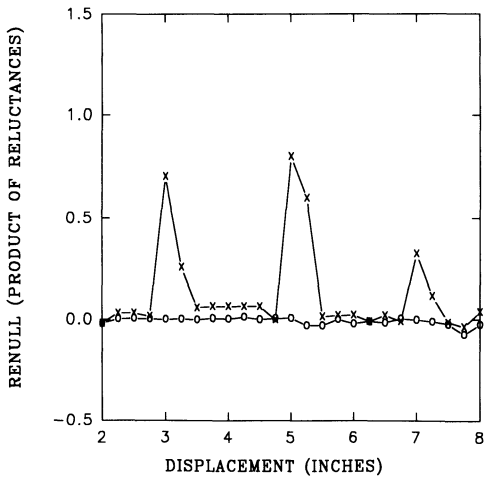

Fig. 8A. Scan of simulated hidden corrosion on the outside of the inside plate of seam.

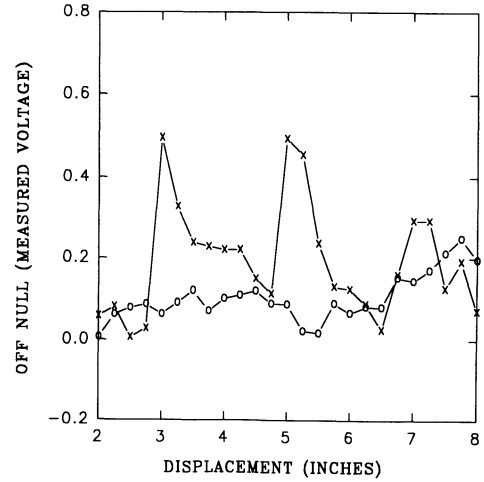

Fig. 8B. Scan of simulated hidden corrosion on the outside of the inside plate of seam.

of the three simulated corrosion losses which seems to indicate that at the standard null point (x=2 on Scan A) the bridge was biased far from what would have been the average of Scan B had there been no simulated corrosion losses on Scan B.

In Figs. 8A and 8B, renull and off-null scans are shown for simulated corrosion losses on the outside of the inner plate of the seam (the configuration shown in Fig. 2c). Again, the 19, 13, and 7 percent losses appear at x=3, 5, and 7 inches in both the processed renull (Fig. 8A) and the off-null scans (Fig. 8B). Again processing the scan (Fig. 8A) removes excursions seen on the unprocessed, unflawed, off-null scan (Fig. 8B).

The further away the flaws are, the more difficult they should be to find. In this situation, the plate configuration is represented by configuration of Fig. 2d. The scans of this configuration are shown in Figs. 9A and 9B. The percentage losses now become 9, 6, and 3 because of the double layer of metal. The device clearly responds to the 9 and 6 percent losses in both the processed and unprocessed results, but there is little or no response to the 3 percent loss.

The plates were not flat, and gaps of approximately 0.005 inches occurred between the plates in the vicinity of Scan B. No measurements were made of these gaps and no tests were carried out to see how these gaps affected the results. However, trends seen in some of the unflawed scans seem to indicate the presence of these gaps.

It appears that the renull mode of the bridge is most sensitive to the hidden-corrosion flaws. However, the experiment suggests that biasing the bridge on one of

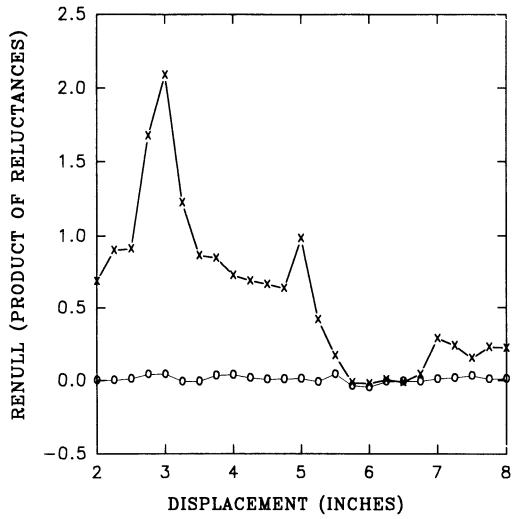

Fig. 9A. Scan of simulated hidden corrosion on the inside of the inside of seam.

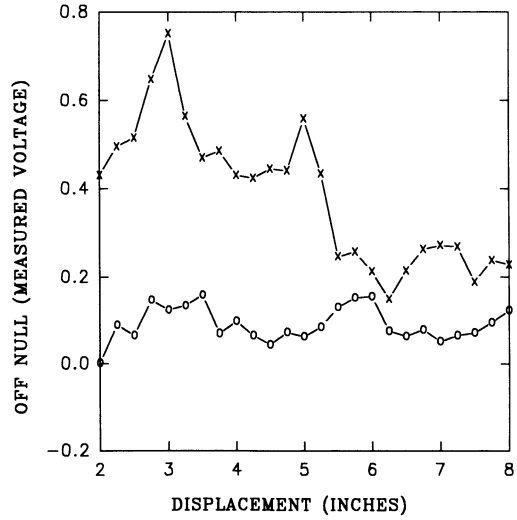

Fig. 9B. Scan of simulated hidden corrosion on the inside of the inside plate of seam.

the slopes on either side of the null seen in Fig. 3 might improve the off-null voltage response. Under any circumstances, present operation of the bridge seems to detect simulated corrosion losses of 7 percent or more whether such losses occur in the seams or under the skin. Consequently, the technique shows considerable promise for detection of hidden corrosion under the skin and in the seams of aging aircraft.

The technique described here is operated at a larger value of lift off (0.008 inches) than is normally used in conventional eddy-current inspections. With such a large lift off, the presence of paint on the surface is a factor which can be ignored except as it affects variable lift off. Higher values of lift off may even be possible and could minimize problems encountered with variable lift off as a result of surface roughness. The technique of processing the data obtained with this method shows some promise of cancelling the effects of surface roughness. Finally, it should be emphasized that this was a first effort at obtaining data on aircraft seams. No effort was made to optimize results either through a choice of lift off, through a choice of input ampturns to the bridge, or choice of frequency. Yet the results compare very favorably to those presented in the other paper examining aircraft seams in this volume [1].

REFERENCES

1. See for example, S. Mitra, P.S. Urali, J.H. Rose, and J.C. Moulder, "Eddy Current Measurement of Corrosion-Related Thinning in Aluminum Lap Splices," this volume.
2. For partial bibliography, see articles listed by W.F. Schmidt and O.H. Zinke, "Reluctance Variation as a Result of Lift off for an AC Magnetic Bridge," this volume.
3. O.H. Zinke and W.F. Schmidt, "Measurement of Stress with AC Magnetic Bridges," *Review of Progress in Quantitative Nondestructive Evaluation* Vol. i, 2051, edited by D.O. Thompson and D.E. Chimenti (Plenum Press, New York, 1989).

4. O.H. Zinke and R.W. Derby, "Nondestructive Measurements of Plating Thicknesses of Copper and Nickel on Shim Stock and of Nickel on Steel," *Review of Progress in Quantitative Nondestructive Evaluation* Vol. 11, 1953, edited by D.O. Thompson and D.E. Chimenti, (Plenum Press, New York, 1992).
5. O.H. Zinke and W.F. Schmidt, "Theory of AC Magnetic Circuits," to appear IEEE Transactions on Magnetics.